STRUCTURE AND THERMAL TRANSFORMATIONS OF IMOGOLITE STUDIED BY ^{29}Si AND ^{27}Al HIGH-RESOLUTION SOLID-STATE NUCLEAR MAGNETIC RESONANCE

K. J. D. MacKenzie, M. E. Bowden, I. W. M. Brown,
AND R. H. Meinhold

Chemistry Division, Department of Scientific and Industrial Research
Private Bag, Petone, New Zealand

Abstract—Solid-state nuclear magnetic resonance (NMR) spectroscopy, thermal analysis, and X-ray powder diffraction data on the tubular, hydrous aluminosilicate imogolite were found to be fully consistent with a previously proposed crystal structure consisting of a rolled-up, 6-coordinate Al–O(OH) sheet, bonded to isolated orthosilicate groups. The calculated ^{29}Si chemical shift of this structure agreed with the observed shift within 3 ppm. Thermal dehydroxylation of the Al–O(OH) sheet produced predominantly NMR-transparent 5-coordinate Al, but a few 4- and 6-coordinate sites and some residual hydroxyl groups may also have formed, as shown by NMR spectroscopy. Changes in the ^{29}Si NMR spectrum on dehydroxylation suggest a condensation of the orthosilicate groups, but steric considerations rule out bonding between adjacent silicons. To account for these observations, an alternative mechanism to orthosilicate condensation has been proposed, involving the fracture and unrolling of the tubes, followed by the condensation of fragments to form a layer structure. The layer structure has a calculated ^{29}Si chemical shift of -95.6 ppm, in good agreement with the observed value of -93 ppm.

Key Words—Aluminosilicate gel, Crystal structure, Dehydroxylation, Imogolite, Nuclear magnetic resonance, Thermal treatment, X-ray powder diffraction.

INTRODUCTION

Imogolite is the name given to a hydrated aluminosilicate having characteristic tubular morphology and an Al_2O_3/SiO_2 ratio of about 1. A structure proposed by Wada (1967) consisting of a continuous tetrahedral Si–O chain linking two octahedral Al–OH chain units was subsequently modified by Wada and Yoshinaga (1968) to take into account the 8.40-Å repeat distance by postulating the octahedral chains to be gibbsite-like (Figure 1A). A similar gibbsite chain or ribbon was suggested by Russell *et al.* (1969), but their gibbsite chain was linked by isolated Si_2O_7 groups rather than being a continuous silicate chain proposed by Wada and Yoshinaga (1968). The presence of orthosilicate SiO_4 groups was later demonstrated by Cradwick *et al.* (1972), who deduced a structure (Figure 1B) that accounted for the known morphology, chemical composition, and electron diffraction pattern.

A knowledge of the structural features and heating behavior of imogolite is of particular interest because of current discussion about the structure of the related, but more poorly crystalline, allophanes. One school of thought (e.g., Wada and Wada, 1977) regards these poorly crystalline allophanes as being composed of hollow spherules, the walls of which have a structure similar to a defect-containing kaolinite (Brindley and Fancher, 1970). An alternative view is that allophanes have wall structures made up of imogolite structural units, in which the framework is based on the octahedral Al sheet (Parfitt and Henmi, 1980).

One useful strategy for studying the structures of poorly crystalline materials is to transform them by heating into more highly crystalline phases and to monitor the changes by X-ray powder diffraction, or, more recently, solid-state nuclear magnetic resonance (NMR) with magic-angle spinning (MAS). This paper reports such a study of imogolite, which in a subsequent paper will be compared with various allophanes, with the aim of addressing the question of structural similarity.

On heating, imogolite loses physically adsorbed water at <200°C (Russell *et al.,* 1969), but the structural (hydroxyl) water is more thermally stable than in allophane (Russell *et al.,* 1969), being lost in a discrete endothermic event at about 400°C (Wada and Yoshinaga, 1968). Although Russell *et al.* (1969) reported that the tubular morphology is unchanged by heating to 700°C, Van der Gaast *et al.* (1985) observed that dehydroxylation at 500°C was accompanied by a breakdown of the tubes.

High-resolution solid-state ^{29}Si and ^{27}Al NMR was used by Goodman *et al.* (1985) to confirm the essentially 6-coordinate environment of the Al in imogolite and in "proto-imogolite," a non-tubular aluminosilicate having an incompletely formed imogolite structure. The sharp ^{29}Si resonance reported at -78 ppm by both Goodman *et al.* (1985) and Barron *et al.* (1982) is qualitatively consistent with isolated silicate groups coordinated through oxygen atoms to three aluminum atoms and one proton, as required by the structure of Cradwick *et al.* (1972). The effect of dehydration on the ^{29}Si and ^{27}Al spectra was studied by Wilson *et al.*

(1988), but difficulties remain in relating the observed results to the crystallography of the imogolite.

The aim of the present work was to address the outstanding crystallographic problems relating to structural changes induced in imogolite by the removal of water and subsequent recrystallization, thereby providing information about the structure of the unheated mineral. The major experimental techniques used were solid-state NMR spectroscopy, X-ray powder diffraction (XRD), and thermal analysis.

EXPERIMENTAL

The imogolite was from the Kitakami Pumice Bed, Japan, and was kindly supplied by K. Wada. The collection and purification of this material, designated Ki-G, has been described elsewhere (Van der Gaast *et al.*, 1985). Chemical analysis by atomic absorption spectrometry gave the following composition: SiO_2, 23.61%; Al_2O_3, 36.00%; TiO_2, 0.06%; Fe_2O_3, 0.20%; MgO, 0.06%; CaO, 0.18%; MnO, 0.01%; Na_2O, 1.49%; K_2O, 0.10%, H_2O (total), 37.6%. The SiO_2/Al_2O_3 mole ratio (1.11) is close to that of ideal imogolite (1.0).

The infrared spectrum supplied by K. Wada is similar to published spectra (Russell *et al.*, 1969), and the XRD pattern is identical to that reported for imogolite from the same location (Brown, 1980), with the same low-angle features as found by Van der Gaast *et al.* (1985).

Thermal analysis was carried out in air at a heating rate of 10°C/min using a Stanton TG770 micro thermobalance and a Stone model 202 differential thermal analyzer. The sample for solid-state NMR was progressively heated in a platinum foil lined boat to temperatures chosen with reference to the thermal analysis curves. The dwell time at each temperature was 15 min. The solid-state NMR spectroscopy was carried out using a Varian XL-200 spectrometer at magic-angle spinning speeds of 2–2.5 kHz. The magic angle was set using KBr spinning side bands. The following approximate values for the relaxation parameters in unheated imogolite were determined: $T_1(H) = 9$ ms, $T_{1\rho}(H) = 5$ ms, $T_{SiH} = 0.8$ ms, $T_1(Si) = 0.7$ s. For ^{29}Si cross-polarization experiments a recycle delay of 0.1 s and a contact time of 3 ms were used. For the ^{29}Si Bloch decay experiments a delay of 3 s was used between 90° pulses of 16 μs with high-power proton decoupling during acquisition. ^{27}Al spectra were obtained using a π/12 pulse of 2 μs, with a recycle delay of 0.15 ($\gg T_1$). NMR-visible Al was quantified by comparison with an internal standard of α-Al_2O_3. After each heating, the sample was also examined by XRD, and, where crystalline phases had formed at higher temperatures, careful lattice parameter measurements were made, using a Philips computer-controlled diffractometer with CoKα radiation, a graphite monochromator, and elemental Si as the internal angular calibrant.
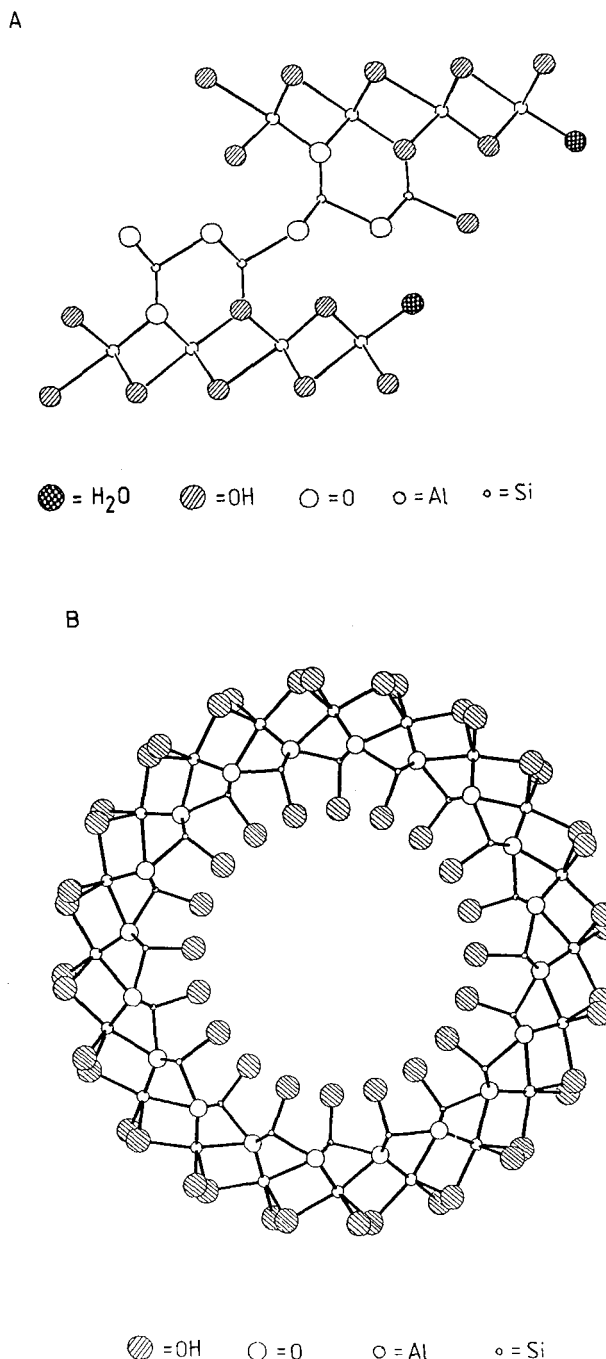

Figure 1. Computer-generated diagrams of previously suggested imogolite structures. (A) "Chain" structure of Wada and Yoshinaga (1968) viewed down chain axis. Each Al is 6-coordinate, with two bonds perpendicular to plane of paper. (B) Structure of Cradwick *et al.* (1972) viewed down tube axis.

RESULTS AND DISCUSSION

The thermal analysis traces (Figure 2) are characteristic of imogolite, having an endothermic weight loss of about 25.5% hydration water <200°C, followed by a 13% endothermic weight loss due to dehydroxylation,
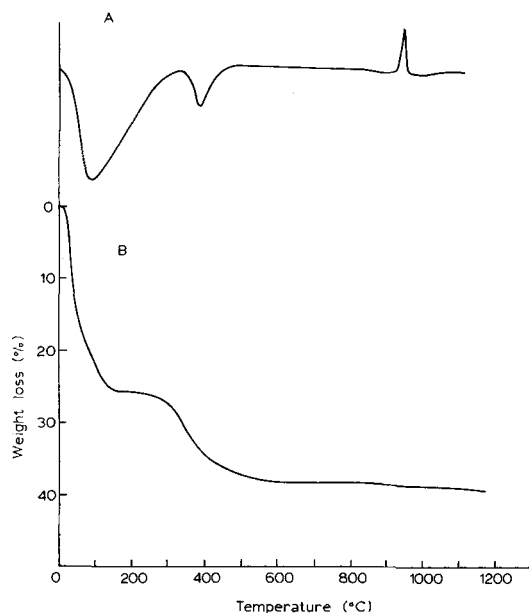
Figure 2. (A) Differential thermal analysis trace of Japanese imogolite, sample Ki-G. Heating rate = 10°C/min, in air. (B) Thermogravimetric curve, heating rate = 10°C/min, in air.

which reaches maximum rate at about 400°C. The XRD pattern was unchanged by the removal of hydration water <300°C, although the shape of the broad, intense combination reflection at about 14–16 Å changed, apparently because of the progressive loss of a component at about 13.7 Å. At 400°C, the intensities of all the XRD reflections decreased markedly, the weakest reflections being lost altogether; the pattern at this stage strongly resembled that of non-tubular allophane. Complete dehydroxylation at 600°C resulted in a totally X-ray-amorphous phase, which gradually lost additional weight (0.75%) to about 960°C, the temperature of the exothermic recrystallization of mullite (Figure 2). Heating to higher temperatures improved the mullite crystallinity and further decreased the small amount of the X-ray-amorphous component, as detected by the weak, broad background curvature in the XRD trace of the sample heated to 1000°C. The cell volume of the mullite formed at 1200°C was 167.2 Å^3, corresponding to a composition of 60 mole % Al_2O_3, according to the relationship of Cameron (1977).

The solid-state NMR spectra of samples heated to various temperatures are shown in Figure 3. ^{29}Si spectra were obtained both by Bloch decay and by cross-polarization (CP), which detects only those silicon atoms in proximity to protons. CP spectra were obtained for all samples heated <700°C, above which temperature no protons remained. The CP spectra were identical to those obtained by Bloch decay, but were more intense. After correction for relaxation effects the ratio of the CP to Bloch decay intensities in unheated imogolite suggested that substantially all the Si was cross-
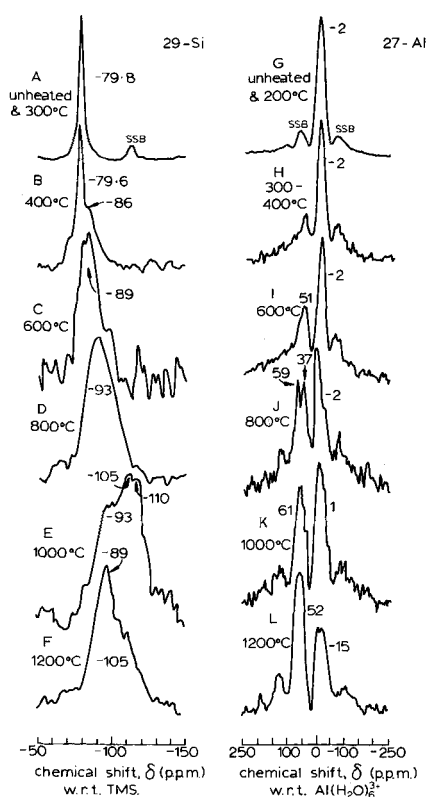

Figure 3. High-resolution ^{29}Si and ^{27}Al solid-state nuclear magnetic resonance spectra of imogolite Ki-G unheated and heated in air to various temperatures for 15 min. Spinning side bands marked SSB.

polarized. The CP peak intensities decreased on heating the samples, as would be expected from the loss of Si–OH groups. This intensity decrease, however, may also have been due in part to changes in the ^{1}H relaxation parameters (e.g., $T_{1\rho}(H)$, T_{SiH}) caused by changes in molecular motion that accompanied the removal of free water.

The removal of hydration water alone did not change the chemical shift of the ^{29}Si peak (Figure 3A), but on partial dehydroxylation at 400°C, a shoulder appeared at about −86 ppm (Figure 3B), which eventually became the broad resonance of the fully dehydroxylated phase (Figure 3C). These spectral changes accompanying dehydroxylation were identical to those found by Wilson et al. (1988). The dehydroxylate spectrum centered at −89 to −93 ppm was identical to that of unheated, natural allophane and synthetic 1:1 aluminosilicate gels (Goodman et al., 1985). Recrystallization at 1000°C resulted in the appearance of a broad peak at −110 ppm (Figure 3E), corresponding to the separation of some X-ray-amorphous silica (Smith and Blackwell, 1983), in addition to the characteristic mullite resonance at −93 ppm. An additional feature at about −105 ppm was similar to a broad peak found by Komarneni et al. (1986) in single-phase alumino-

silicate gels of mullite composition and attributed by them to the substitution of some Al(IV) for Si. The mullite resonance shifted slightly to -89 ppm and became dominant after further heat treatment of the sample (Figure 3F).

The ^{27}Al NMR spectra are shown in Figures 3G–3L. Calibration of the integrated peak intensities with respect to the intensity produced by a known amount of Al in an external standard of α-Al$_2$O$_3$ indicated that the NMR experiment detected all the Al present in the unheated sample, but that the loss of both hydration and hydroxyl water decreased the amount of Al detected in the heated samples (Figure 4). Recrystallization at higher temperatures only slightly improved the Al detection level, consistent with the dehydroxylation behavior of other hydrated aluminosilicates studied by solid-state NMR (MacKenzie *et al.,* 1985a, 1985b, 1987; Brown *et al.,* 1987).

The ^{27}Al spectrum of unheated imogolite (Figure 3G) indicated predominantly octahedral Al, as reported by Goodman *et al.* (1985) and Wilson *et al.* (1988). The relatively low magnetic field of 4.7 Tesla and the spinning speeds available for the present work were insufficient to allow the small amount of tetrahedral Al previously reported by Goodman *et al.* (1985) to be distinguished from the spinning side bands. The slight asymmetry in the spinning side bands, which may have reflected this tetrahedral component (Figure 3G), was unaffected by the loss of hydration water, but on dehydroxylation, the non-octahedral component markedly increased, as evidenced by the growth of a resonance at 51 ppm (Figure 3I). After dehydroxylation, but prior to recrystallization, the amount of Al visible was small and resulted in poor signal-to-noise, but peaks appeared to be present at about 37 and 59 ppm (Figure 3J). Similar results were found for both dehydroxylated pyrophyllite and metakaolinite by MacKenzie *et al.* (1985a, 1985b), who suggested that these two peaks represented Al in slightly different tetrahedral environments, although the peak at 37 ppm could possibly have been due to a more regular 5-coordinated Al site (Alemany and Kirker, 1986). The separation of these sites was lost on recrystallization of the sample (Figure 3K), which was accompanied by a further increase in the proportion of detectable tetrahedral Al (Figure 4B) and a change in the octahedral chemical shift to -15 ppm (Figure 3L).

Implications for the structure of imogolite and its dehydroxylate

Previous work on several aluminosilicate minerals (e.g., MacKenzie *et al.,* 1985a, 1985b) has shown the ^{29}Si chemical shift δ to be related to the mean Si–O–Si(Al) angle θ by the relationship:

$$\delta = -176.65 - 55.821 \sec \theta. \qquad (1)$$

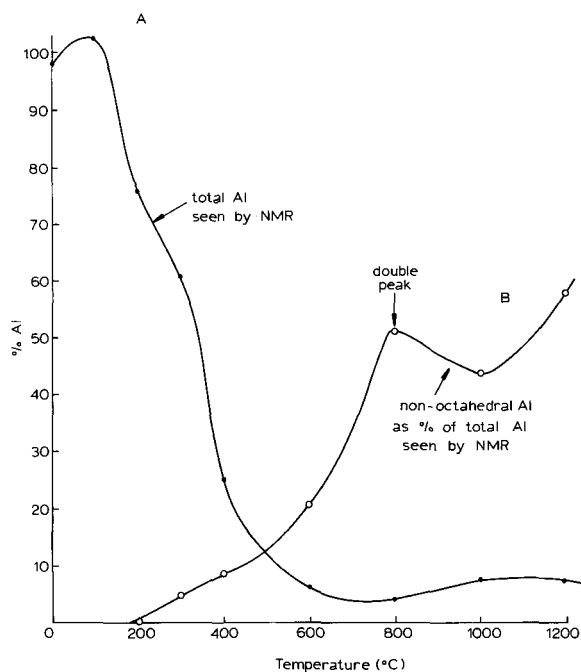Because this relationship is based on angles derived

Figure 4. (A) Percentage of nuclear magnetic resonance visible ^{27}Al signal in imogolite Ki-G as a function of heating temperature. (B) Intensity of non-octahedral ^{27}Al nuclear magnetic resonance signal expressed as percentage of total nuclear magnetic resonance visible ^{27}Al for imogolite Ki-G heated to various temperatures for 15 min.

from experimentally determined crystal structures, it takes into account the contribution of adjacent Al atoms. Furthermore, because the *mean* tetrahedral angle θ is used, the method is suitable for systems in which more than one Al atom is coordinated through oxygen to the silicon concerned (MacKenzie *et al.,* 1985a). This method has predicted within about 2 ppm the ^{29}Si chemical shifts of several minerals for which precise crystal structures are available, and it has also been used to deduce structural information for noncrystalline dehydroxylated aluminosilicates from their NMR chemical shifts (MacKenzie *et al.,* 1985a, 1985b).

Based on the imogolite structure proposed by Cradwick *et al.* (1972), computer simulations were made of both the 20-unit (C_{20h}) and 24-unit (C_{24h}) tubes, from which the mean tetrahedral angles were computed. By substituting these into Eq. (1), mean chemical shifts of -82.4 and -82.9 ppm were predicted for the C_{20h} and C_{24h} structures, respectively. These values are sufficiently close to the experimental chemical shift of -79.8 ppm to engender confidence in the structure of Cradwick *et al.* (1972). The correct placement of water and hydroxyl groups in this structure is also confirmed by the spectral changes induced by heating to 100°C, which decreased the intensity of the ^{29}Si CP spectrum, but not the ^{27}Al spectrum. This arrangement is consistent with the location of Si-containing units towards the inside of the tubes, in close proximity to the water

enclosed by the tubes, thereby influencing ^{1}H hydroxyl relaxation by spin diffusion from the water protons.

For example, similar chemical-shift calculations were carried out for the chain structure proposed earlier by Wada and Yoshinaga (1968). Computer simulation of this structure indicated at least three different distorted Si sites with improbable Si–O bond lengths ranging from 1.43 to 1.92 Å and bond angles that should have resulted in chemical shifts well downfield from the observed single resonance. Thus, from crystallographic and NMR points of view, the structure of Cradwick et al. (1972) is much superior to previous structures; however, dehydroxylation of the Cradwick structure poses crystallographic problems. The perspective of Figure 1B suggests that the most obvious method of dehydroxylating the isolated SiO$_3$OH units is to condense them into a continuous sheet, as shown in Figure 11 of Wilson et al. (1988). Computer simulation, however, clearly indicated that such a condensation is extremely unlikely, inasmuch as the neighboring silicate units in Figure 1B are displaced by 4.2 Å in the c-direction (perpendicular to the plane of the paper). The shortest Si–Si distance in this structure is 3.94 Å, considerably in excess of the longest distance (3.27 Å) found in a survey of 141 silicon sites in silicates and silicas (O'Keefe and Hyde, 1978).

To bridge these silicon atoms requires a minimum Si–O bond length of 1.97 Å, again considerably longer than the maximum mean bond length (1.654 Å) found in 314 silicate tetrahedra (Baur, 1978). Furthermore, the resulting silicate units would be extremely distorted from tetrahedral symmetry, the oxygen bridge making an Si–O–Si angle of 180°, which, according to a statistical analysis by O'Keefe and Hyde (1978), equates to an Si–O length of 1.58–1.63 Å. Intra-tube condensation of this type is further militated against by the rigidity of the tubular structure, which confers considerable thermal stability compared with allophane or gibbsite. Dehydroxylation of the Al–OH layer poses no such steric difficulty and could proceed directly with formation of predominantly 5-coordinated Al (4-coordinated Al would not be the principal product, as it would if the orthosilicate groups condensed as shown in Figure 11 of Wilson et al. (1988)).

To resolve this structural problem, two possibilities must be considered: (1) that the imogolite structure of Cradwick et al. (1972) is incorrect, or (2) that dehydroxylation of the Si–OH groups proceeds by a mechanism involving tube fracture. Because the structure of Cradwick et al. (1972) accounts very satisfactorily for all the known experimental results, including the solid-state NMR data, and gives calculated ^{29}Si chemical shifts in good agreement with the observed value, possibility (1) does not appear correct. No way exists, however, to adjust this structure to bring the silicate units within bonding distance, even by making radical changes to the disposition of the silicate groups and/

or the gibbsite-like sheet. If the structure is essentially correct, dehydroxylation of the Si–OH groups could have proceeded by cleavage of the tubes, which may have been initiated by dehydroxylation of some of the Al–OH groups (Wilson et al., 1988). As shown schematically in Figure 5, at least two cleavage schemes may be envisaged, leading to different dehydroxylated structures.

In Figure 5A cleavage exists across the diameter, the consequent release of circular constraint causing the two resulting tube halves to flatten, bringing the diametrically opposing Si–OH groups into registration and allowing hydroxyl elimination between them, with the formation of a repeating layer sequence [Al, Si, Si, Al]. Alternatively, tube rupture might be considered to occur at only one point on the circumference (Figure 5B); here, the unrolled tube could interact with an adjacent tube similarly unrolled. Hydroxyl elimination would thus be between Si–OH groups of one tube and undehydroxylated Al–OH groups of the second tube, resulting in a repeating layer sequence [Al, Si, Al, Si].

Computer simulation of the two resulting layer structures was carried out by first unrolling the tubular structure of Cradwick et al. (1972) around the oxygen plane. Interestingly, the ^{29}Si chemical shift of the flattened tube, calculated from Eq. (1) by substituting the calculated mean tetrahedral angle, was −81.1 ppm, not very different from that calculated for the tubes (−82.4 and −82.9 ppm). This similarity indicates that the interatomic geometry, which establishes the chemical shift, was not particularly influenced by the curvature of the tubes. Condensation of two tube fragments as in Figure 5A leads to the layer structure shown in Figure 6A, in which the mean Si–O–Si(Al) angle is 133.5°, corresponding to a calculated ^{29}Si chemical shift of −95.6 ppm. These values are in reasonable agreement with the observed centroid of the broad ^{29}Si resonance of imogolite dehydroxylate (−93 ppm). By contrast, the condensation scheme of Figure 5B leads to the layer structure of Figure 6B, in which the mean Si–O–Si(Al) angle is 125.32°, corresponding to a calculated ^{29}Si chemical shift of −80.1 ppm.

Thus, the structure shown in Figure 6B is less likely, both on the basis of its calculated chemical shift and because it requires the presence in each unrolled tube of a significant concentration of Al–OH groups in close proximity, which may be inconsistent with the postulated tube unrolling mechanism that requires the destruction of such groups. The width of the observed ^{29}Si resonance in imogolite dehydroxylate suggests significant variations in the mean tetrahedral angle. As in dehydroxylated kaolinite and pyrophyllite, these variations most probably arose from differences in the disposition of the aluminum atoms after dehydroxylation, although the presence of a small component of the structure in Figure 6B could have contributed to the downfield portion of the resonance envelope.
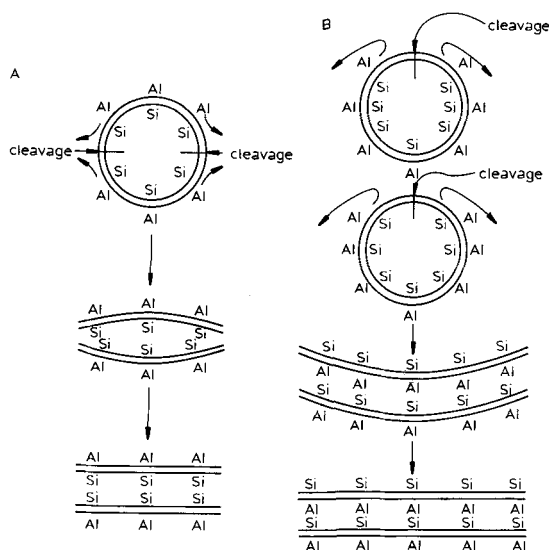
Figure 5. Schematic diagram of two possible fracture mechanisms for dehydroxylating imogolite tubes. (A) Single-tube cleavage with condensation of two fragments. (B) Two-tube cleavage and condensation.
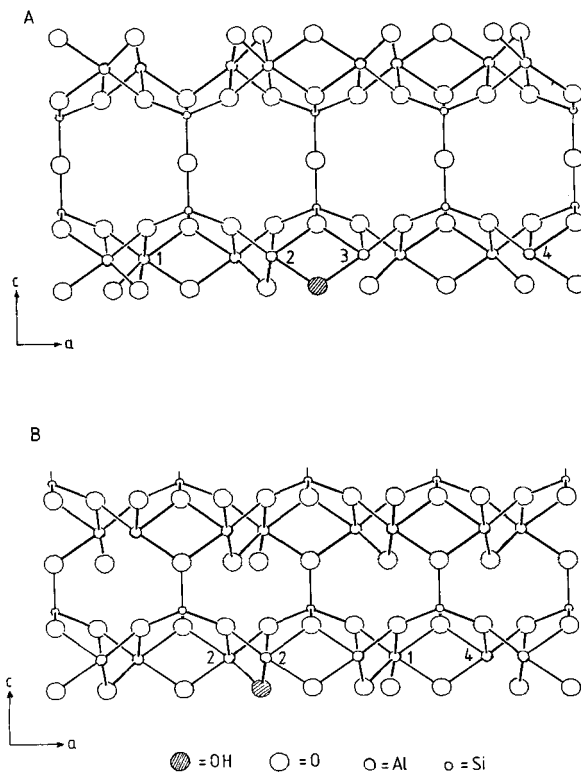

Figure 6. Computer-generated structures of possible layer structures of dehydroxylated imogolite, resulting from (A) single-tube fracture mechanism of Figure 5A, and (B) two-tube mechanism of Figure 5B. Views are along b-axis. Al sites marked 1–4 in lower Al–O sheets of each structure correspond to those indicated in plan view of Figures 7A and 7B, respectively, the sections being taken along the dot-and-dashed line.

In the condensation schemes shown in Figures 5A and 5B, dehydroxylation of the Al–OH layer can proceed readily, as shown in Figures 7A and 7B, respectively, from which the Si atoms are omitted for clarity. Elimination of the hydroxyl pairs joined by broken lines shown in Figures 7A and 7B with the loss of the groups marked X leads to predominantly 5-coordinated Al, although a few other sites may exist, such as 6- and 4-coordinate sites marked 1 and 4, respectively. Furthermore, such a scheme can account for the experimentally observed retention of a few hydroxyls, which became isolated and were unable to condense with near neighbors (Figure 7). The presence of residual hydroxyls will give rise to sites which are not fully anhydrous (sites 2 and 3, Figure 7A). Previous work (MacKenzie *et al.*, 1985a) suggests that the 5-coordinate sites will generally not be detected by NMR whether fully anhydrous or not, but the two weak experimentally observed 4-coordinate Al resonances (Figure 3J) could have arisen from the two different 4-coordinate sites 3 and 4 (Figure 7A). In Figure 7B, corresponding to the less favored scheme of Figure 5B, the options for hydroxyl elimination are more limited because of the need for some of the Al–OH groups to condense with the Si–OH groups. Nevertheless, the scheme shown in Figure 7B allows for the formation of some sites of coordination other than 5.

A dehydroxylation scheme such as shown in Figures 5A, 6A, and 7A is consistent with all the known experimental facts and provides a satisfactory mechanism for the development of the condensed layer structure, which is a necessary precursor to the high-temperature phases. Such a mechanism, however, depends on cleavage of the tubes at an early stage, although this is incompatible with the observation of Russell *et al.* (1969) that the tubular structure survives dehydroxylation at 700°C. More recent work (Van der Gaast *et al.*, 1985, Wilson *et al.*, 1988) suggests that breakdown of the tubes may have begun at about the onset of dehydroxylation, even though the threadlike habit was preserved in the early stages.

CONCLUSIONS

1. Solid-state ^{29}Si and ^{27}Al NMR measurements of imogolite suggest a structure containing an octahedrally coordinated Al–O(OH) sheet associated with isolated silicate groups, as in the structure proposed by Cradwick *et al.* (1972). The ^{29}Si chemical shift for such a structure, calculated from the mean tetrahedral angle by the secant relationship, agrees within 3 ppm with the observed chemical shift and is virtually independent of the curvature of the imogolite tube.

2. On dehydroxylation, at least 90% of the Al sites in imogolite become too distorted to be NMR-visible;
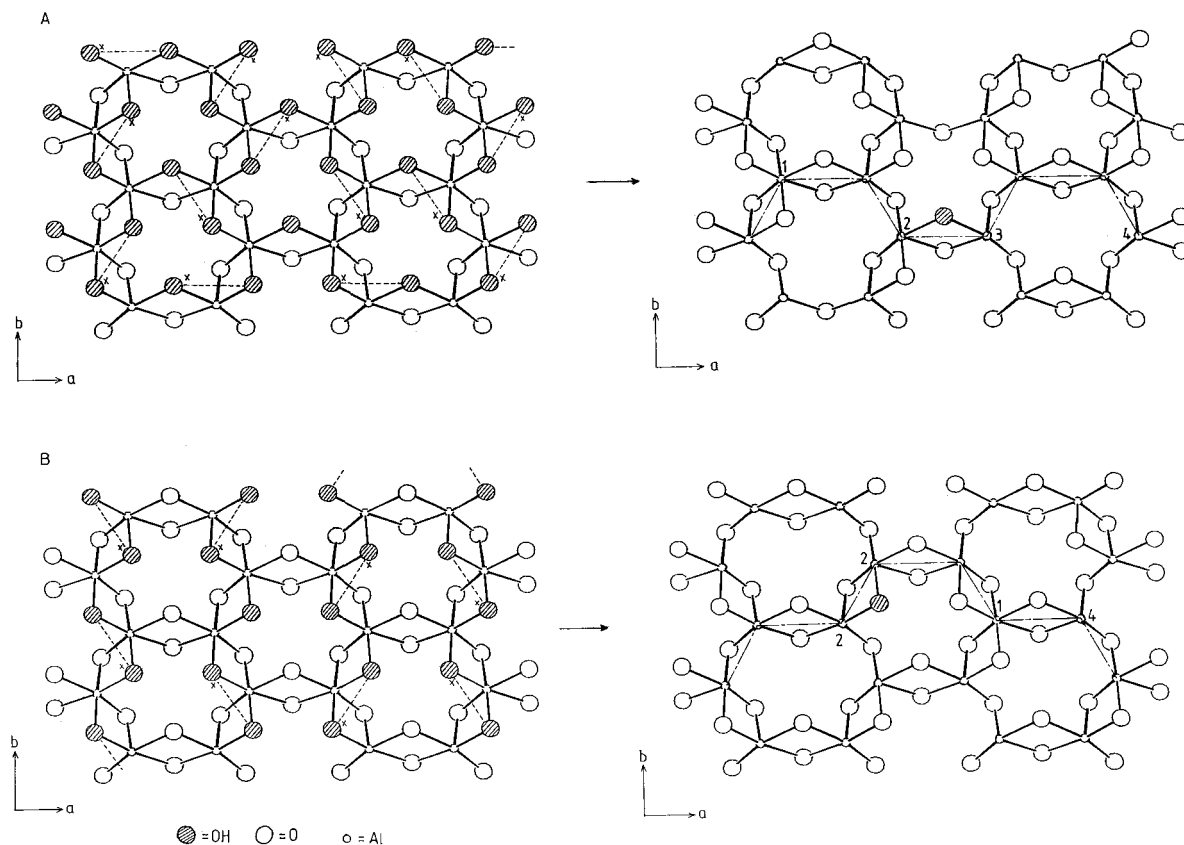
Figure 7.   Schemes for dehydroxylation of Al–OH layers in unrolled imogolite. (A) Single-tube fracture mechanism. (B) Two-tube fracture mechanism. Plan view down the c-axis; silicons are omitted for clarity. Broken lines indicate interacting hydroxyl pairs, the group marked X being eliminated, giving rise to predominantly 5-coordinate sites, but with some sites 6-coordinate (site 1), 4-coordinate (site 4), and 5- and 4-coordinate with residual hydroxyl (sites 2 and 3, respectively).

of those that remain detectable, about half are in non-octahedral sites. These changes can be explained in terms of hydroxyl-elimination schemes, which predict predominantly 5-coordinate (NMR-transparent) Al sites, but with a few 4- and 6-coordinate sites and some isolated hydroxyl groups, which are eliminated only at higher temperatures.

3. Dehydroxylation of imogolite also brings about changes in the ^{29}Si imogolite resonance, which is progressively replaced by a broader, upfield resonance more typical of a condensed silicate framework. Consideration of the interatomic distances in the Cradwick structure rules out the condensation of adjacent silicate units, which would result in unrealistic Si–O bond lengths and angles and which would lead to the early disintegration of the aluminosilicate, contrary to NMR observation.

Alternative mechanisms for eliminating the Si–OH group by invoking tube fracture followed by condensation of the unrolled fragments into layer structures provide an explanation of the NMR observations, particularly for fragments that condense in such a way as to form Si–O–Si bonds. Computer simulation of the resulting layer structure indicates a calculated ^{29}Si chemical shift of −95.6 ppm, in good agreement with the observed shift (−93 ppm). Condensation between more than one tube to form Si–O–Al bonds appears less likely, inasmuch as it results in a calculated chemical shift of −80.1 ppm.

ACKNOWLEDGMENTS

REFERENCES

Alemany, L. B. and Kirker, G. W. (1986) First observation of 5-coordinate aluminium by MAS ^{27}Al NMR in well-characterized solids: *J. Amer. Chem. Soc.* **108**, 6158–6162.

Barron, P. F., Wilson, M. A., Campbell, A. S., and Frost, R. L. (1982) Detection of imogolite in soils using solid state 29-Si NMR: *Nature (Lond.)* **299**, 616–618.

Baur, W. H. (1978) Variation of mean Si–O bond lengths in silicon-oxygen tetrahedra: *Acta Crystallogr.* **B34,** 1751–1756.

Brindley, G. W. and Fancher, D. (1970) Kaolinite defect structures; Possible relation to allophanes: in *Proc. Int. Clay Conf., Tokyo, 1969, Vol. 2,* L. Heller, ed., Israel Univ. Press, Jerusalem, 29–34.

Brown, G. (1980) Associated minerals: in *Crystal Structures of Clay Minerals and Their X-ray Identification,* G. W. Brindley and G. Brown, eds., Mineralogical Society, London, p. 406.

Brown, I. W. M., MacKenzie, K. J. D., and Meinhold, R. H. (1987) The thermal reactions of montmorillonite studied by high resolution solid-state 29-Si and 27-Al NMR: *J. Mater. Sci.* **22,** 3265–3275.

Cameron, W. E. (1977) Composition and cell dimensions of mullite: *Amer. Ceram. Soc. Bull.* **56,** 1003–1011.

Cradwick, P. D. G., Farmer, V. C., Russell, J. D., Masson, C. R., Wada, K., and Yoshinaga, N. (1972) Imogolite, a hydrated aluminium silicate of tubular structure: *Nature Phys. Sci.* **240,** 187–189.

Goodman, B. A., Russell, J. D., Montez, B., Oldfield, E., and Kirkpatrick, R. J. (1985) Structural studies of imogolite and allophanes by aluminium-27 and silicon-29 nuclear magnetic resonance spectroscopy: *Phys. Chem. Mineral.* **12,** 342–346.

Komarneni, S., Roy, R., Fyfe, C. A., Kennedy, G. J., and Strobl, H. (1986) Solid-state 27-Al and 29-Si magic-angle spinning NMR of aluminosilicate gels: *J. Amer. Ceram. Soc.* **69,** C42–C44.

MacKenzie, K. J. D., Brown, I. W. M., Cardile, C. M., and Meinhold, R. H. (1987) The thermal reactions of muscovite studied by high-resolution solid-state 29-Si and 27-Al NMR: *J. Material. Sci.* **22,** 2645–2654.

MacKenzie, K. J. D., Brown, I. W. M., Meinhold, R. H., and Bowden, M. E. (1985a) Thermal reactions of pyrophyllite studied by high-resolution solid-state 27-Al and 29-Si nuclear magnetic resonance spectroscopy: *J. Amer. Ceram. Soc.* **68,** 266–272.

MacKenzie, K. J. D., Brown, I. W. M., Meinhold, R. H., and Bowden, M. E. (1985b) Outstanding problems in the kaolinite-mullite reaction sequence investigated by 29-Si and 27-Al solid-state nuclear magnetic resonance: I. Metakaolinite: *J. Amer. Ceram. Soc.* **68,** 293–297.

O'Keefe, M. and Hyde, B. G. (1978) On Si–O–Si configurations in silicates: *Acta Crystallogr.* **B34,** 27–32.

Parfitt, R. L. and Henmi, T. (1980) Structure of some allophanes from New Zealand: *Clays & Clay Minerals* **28,** 285–294.

Russell, J. D., McHardy, W. J., and Fraser, A. R. (1969) Imogolite: A unique aluminosilicate: *Clay Miner.* **8,** 87–99.

Smith, J. V. and Blackwell, C. S. (1983) Nuclear magnetic resonance of silica polymorphs: *Nature (Lond.)* **303,** 223–225.

Van der Gaast, S. J., Wada, K., Wada, S-I., and Kakuto, Y. (1985) Small-angle X-ray powder diffraction, morphology and structure of allophane and imogolite: *Clays & Clay Minerals* **33,** 237–243.

Wada, K. (1967) A structural scheme of soil allophane: *Amer. Mineral.* **52,** 690–708.

Wada, K. and Yoshinaga, N. (1968) The structure of "imogolite": *Amer. Mineral.* **54,** 50–71.

Wada, S-I. and Wada, K. (1977) Density and structure of allophane: *Clay Miner.* **12,** 289–298.

Wilson, M. A., Wada, K., Wada, S-I., and Kakuto, Y. (1988) Thermal transformations of synthetic allophane and imogolite as revealed by nuclear magnetic resonance: *Clay Miner.* **23,** 175–190.